Supporting Information for

Origin of Asynchronicity in Diels-Alder Reactions

Pascal Vermeeren,*[a] Trevor A. Hamlin,*[a] F. Matthias Bickelhaupt,*[a,b]

[a] Department of Theoretical Chemistry, Amsterdam Institute of Molecular and Life Sciences (AIMMS), Amsterdam Center for Multiscale Modeling (ACMM), Vrije Universiteit Amsterdam, De Boelelaan 1083, 1081 HV Amsterdam, The Netherlands.
E-mail: p.vermeeren@vu.nl, t.a.hamlin@vu.nl, f.m.bickelhaupt@vu.nl

[b] Institute for Molecules and Materials, Radboud University Nijmegen, Heyendaalseweg 135, 6525 AJ Nijmegen, The Netherlands.

Contents

Fig. S6 Activation strain analyses of the artificially constraint synchronous, asynchronous and stepwise Diels-Alder reaction mode (rxn mode) of **B** with **O–H**$^+$ (dot indicates TS) along the IRC projected onto the shorter newly forming a $C_{\mathbf{B}}$•••C_β bond, computed at ZORA-BP86/TZ2P: (a) total energy, (b) strain energy, (c) interaction energy, (d) Pauli repulsion, (e) electrostatic interaction, and (f) orbital interactions.

Fig. S7 Activation strain analyses of the artificially constraint synchronous, asynchronous and stepwise Diels-Alder reaction mode (rxn mode) of **B** with **O** and **O–Li**$^+$ (dot indicates TS) along the IRC projected onto the shorter newly forming a $C_{\mathbf{B}}$•••C_β bond, computed at ZORA-BP86/TZ2P: (a) total energy, (b) strain energy, (c) interaction energy, (d) Pauli repulsion, (e) electrostatic interaction, and (f) orbital interactions.

Fig. S8 (a) Normal and (b) inverse electron demand orbital interaction diagrams with key overlaps and orbital energies, at consistent transition state-like geometries (shorter $C_{\mathbf{B}}$•••C_β bond at 2.186Å), of the artificially constraint synchronous, asynchronous, and stepwise Diels-Alder reaction mode (rxn mode) of **B** with **O–Li**$^+$, computed at ZORA-BP86/TZ2P.

Fig. S9 Normal electron demand orbital interaction diagrams with key overlaps and orbital energies, at consistent transition state-like geometries (shorter $C_{\mathbf{B}}$•••C_β bond at 2.186Å), of the artificially constraint synchronous, asynchronous, and stepwise Diels-Alder reaction mode (rxn mode) of **B** with **O**$^+$, computed at ZORA-BP86/TZ2P.

Fig. S10 Key unoccupied π-MO (isovalue = 0.03 Bohr$^{-3/2}$) computed at the equilibrium structures of (a) **O** and (b) **O–Li**$^+$, where the MO-coefficients of the carbon and oxygen 2p_z atomic orbitals, contributing to the unoccupied orbitals, are shown in the schematic π-MOs, computed at ZORA-BP86/TZ2P.

Fig. S11 Activation strain analyses of the artificially constraint synchronous, asynchronous and stepwise Diels-Alder reaction mode (rxn mode) of **B** with **O** and **O–H**$^+$ (dot indicates TS) along the IRC projected onto the shorter newly forming a $C_{\mathbf{B}}$•••C_β bond, computed at ZORA-BP86/TZ2P: (a) total energy, (b) strain energy, (c) interaction energy, (d) Pauli repulsion, (e) electrostatic interaction, and (f) orbital interactions.

Fig. S12 (a) Normal and (b) inverse electron demand orbital interaction diagrams with key overlaps and orbital energies, at consistent transition state-like geometries (shorter $C_{\mathbf{B}}$•••C_β bond at 2.186Å), of the artificially constraint synchronous, asynchronous, and stepwise Diels-Alder reaction mode (rxn mode) of **B** with **O–H**$^+$, computed at ZORA-BP86/TZ2P.

Fig. S13 Closed-shell orbital interaction diagrams with key overlaps, at consistent transition state-like geometries (shorter $C_{\mathbf{B}}$•••C_β bond at 2.186Å), of the artificially constraint synchronous, asynchronous, and stepwise Diels-Alder reaction mode (rxn mode) of **B** with **O–H**$^+$, computed at ZORA-BP86/TZ2P.

Fig. S14 Key occupied π-MOs (isovalue = 0.03 Bohr$^{-3/2}$) computed at the equilibrium structures of (a) **O** and (b) **O–H**$^+$, where the MO-coefficients of the carbon and oxygen 2p_z atomic orbitals, contributing to the occupied orbitals, are shown in the schematic π-MOs, computed at ZORA-BP86/TZ2P.

Fig. S15 Closed-shell orbital interaction diagrams with key overlaps, at consistent transition state-like geometries (shorter $C_{\mathbf{B}}$•••C_β bond at 2.186Å), of the artificially constraint synchronous, asynchronous, and stepwise Diels-Alder reaction modes (rxn mode) of **B** with **O–Li**$^+$, computed at ZORA-BP86/TZ2P.

Table S3 Cartesian coordinates (in Å), energies (in kcal mol^{-1}), and number of imaginary frequencies of all stationary points, computed at ZORA-BP86/TZ2P.

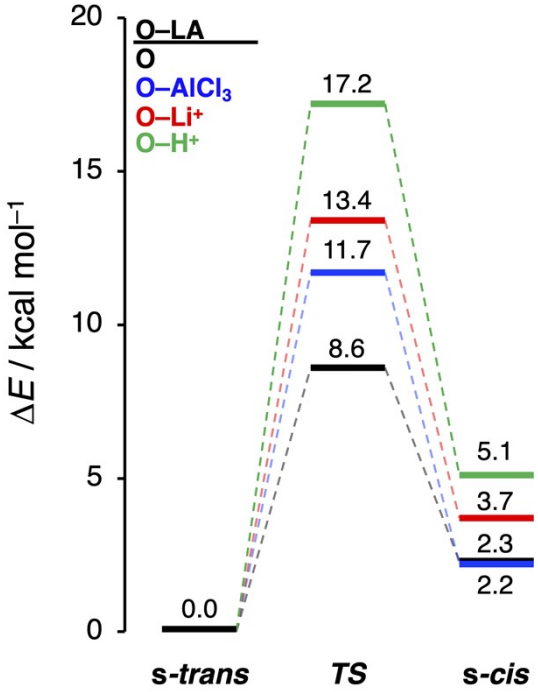

Fig. S1 Stationary points in the energy profile of the rotation around the C=C–C=O dihedral angle of the dienophile, without and with the various Lewis acids, used in this study in which s-*trans* is in all cases the most stable conformation, computed at ZORA-BP86/TZ2P.

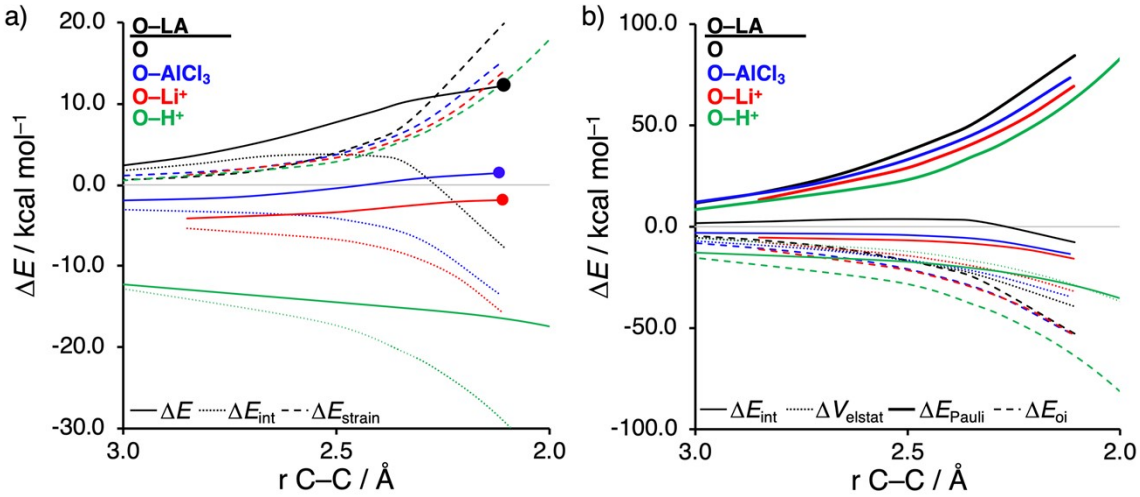

Fig. S2 (a) Activation strain analyses and (b) energy decomposition analyses of the uncatalyzed and Lewis acid-catalyzed Diels-Alder reactions of **B** with **O–LA** along the IRC (from reactants to transition state) projected onto the shorter newly forming $C_{\mathbf{B}}$•••C_β bond, computed at ZORA-BP86/TZ2P.

Table S1 LA•••O=C bond energy decomposition analyses (in kcal mol^{-1}) and distance (in Å) in LA–acrylaldehyde (**O–LA**) complexes.[a]

O–LA	ΔE_{int}	ΔV_{elstat}	ΔE_{Pauli}	ΔE_{oi}	r(LA•••O=C)
O–AlCl$_3$	–35.2	–62.2	71.3	–44.3	1.921
O–Li$^+$	–42.1	–35.7	15.5	–24.9	1.753
O–H$^+$	–204.3	–28.4	0.0	–175.9	0.986

[a] Computed at ZORA-BP86/TZ2P.

Table S2 LA•••O=C bond energy decomposition analyses (in kcal mol^{-1}) and distance (in Å) computed on consistent transition state-like geometries with a $C_{\mathbf{B}}$•••C_β bond length between **B** and **O–LA** of 2.118Å.[a,b]

O–LA	ΔE_{int}	ΔV_{elstat}	ΔE_{Pauli}	ΔE_{oi}	r(LA•••O=C)
O–AlCl$_3$	–49.5	–76.9	85.6	–58.2	1.850
O–Li$^+$	–60.5	–48.1	19.5	–31.9	1.703
O–H$^+$	–238.9	–45.2	0.0	–193.6	0.986

[a] Computed at ZORA-BP86/TZ2P. [b] The interacting fragments are (i) the Lewis acids and (ii) the dienophile and diene.

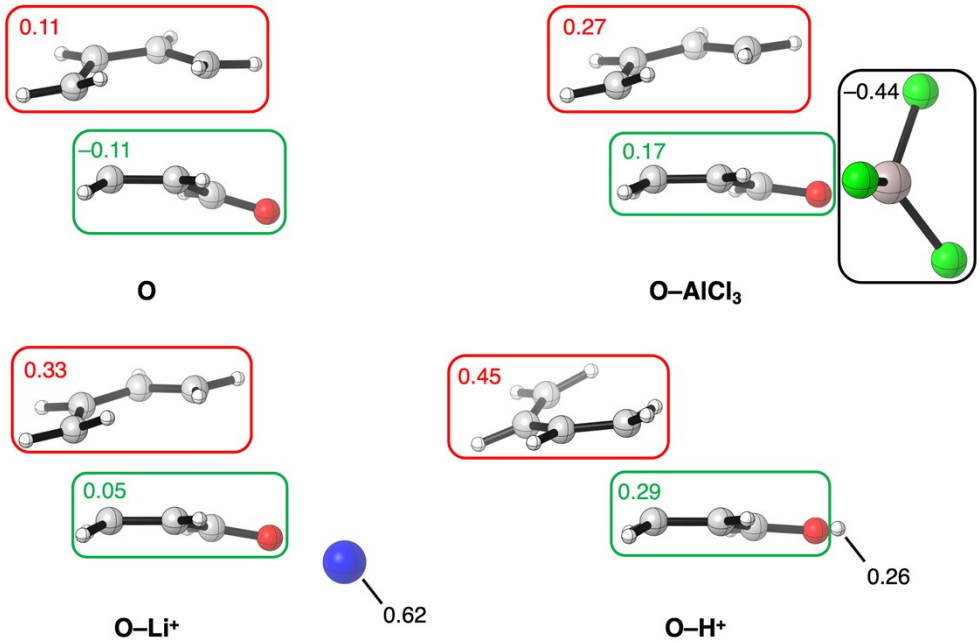

Fig. S3 Voronoi deformation density (VDD) atomic charges (in electrons) of the diene (red), dienophile (green), and Lewis acid (black), computed at consistent transition state-like geometries with a $C_{\mathbf{B}}$•••C_{β} bond length between **B** and **O–LA** of 2.118Å at ZORA-BP86/TZ2P.

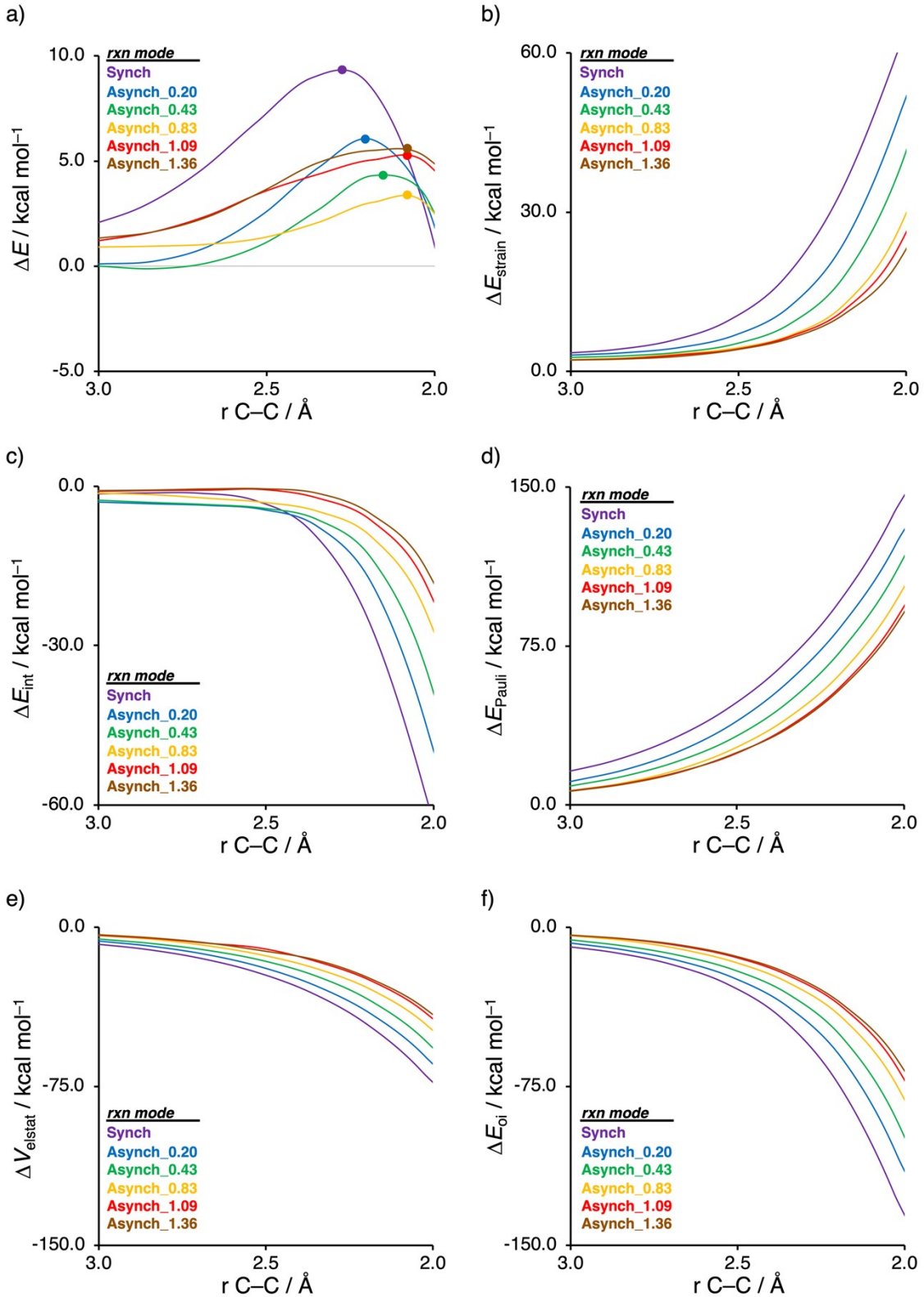

Fig. S4 Activation strain analyses of the artificially constraint synchronous and asynchronous Diels-Alder reaction mode (rxn mode) of **B** with **O–AlCl$_3$** (dot indicates TS) along the IRC projected onto the shorter newly forming a $C_{\mathbf{B}}$•••C_β bond, computed at ZORA-BP86/TZ2P: (a) total energy, (b) strain energy, (c) interaction energy, (d) Pauli repulsion, (e) electrostatic interaction, and (f) orbital interactions.

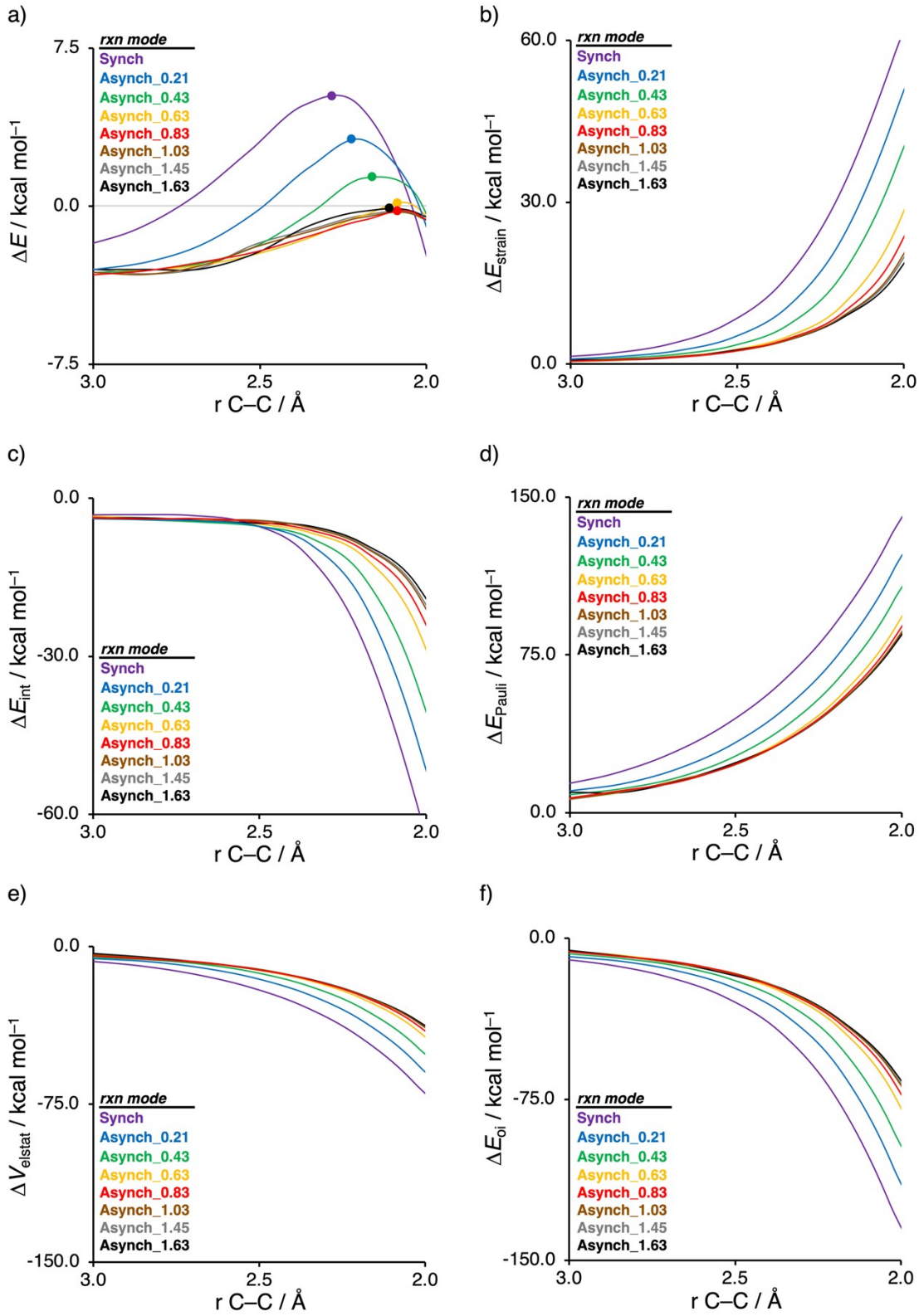

Fig. S5 Activation strain analyses of the artificially constraint synchronous and asynchronous Diels-Alder reaction mode (rxn mode) of **B** with **O–Li**$^+$ (dot indicates TS) along the IRC projected onto the shorter newly forming a $C_{\mathbf{B}}$•••C_β bond, computed at ZORA-BP86/TZ2P: (a) total energy, (b) strain energy, (c) interaction energy, (d) Pauli repulsion, (e) electrostatic interaction, and (f) orbital interactions.

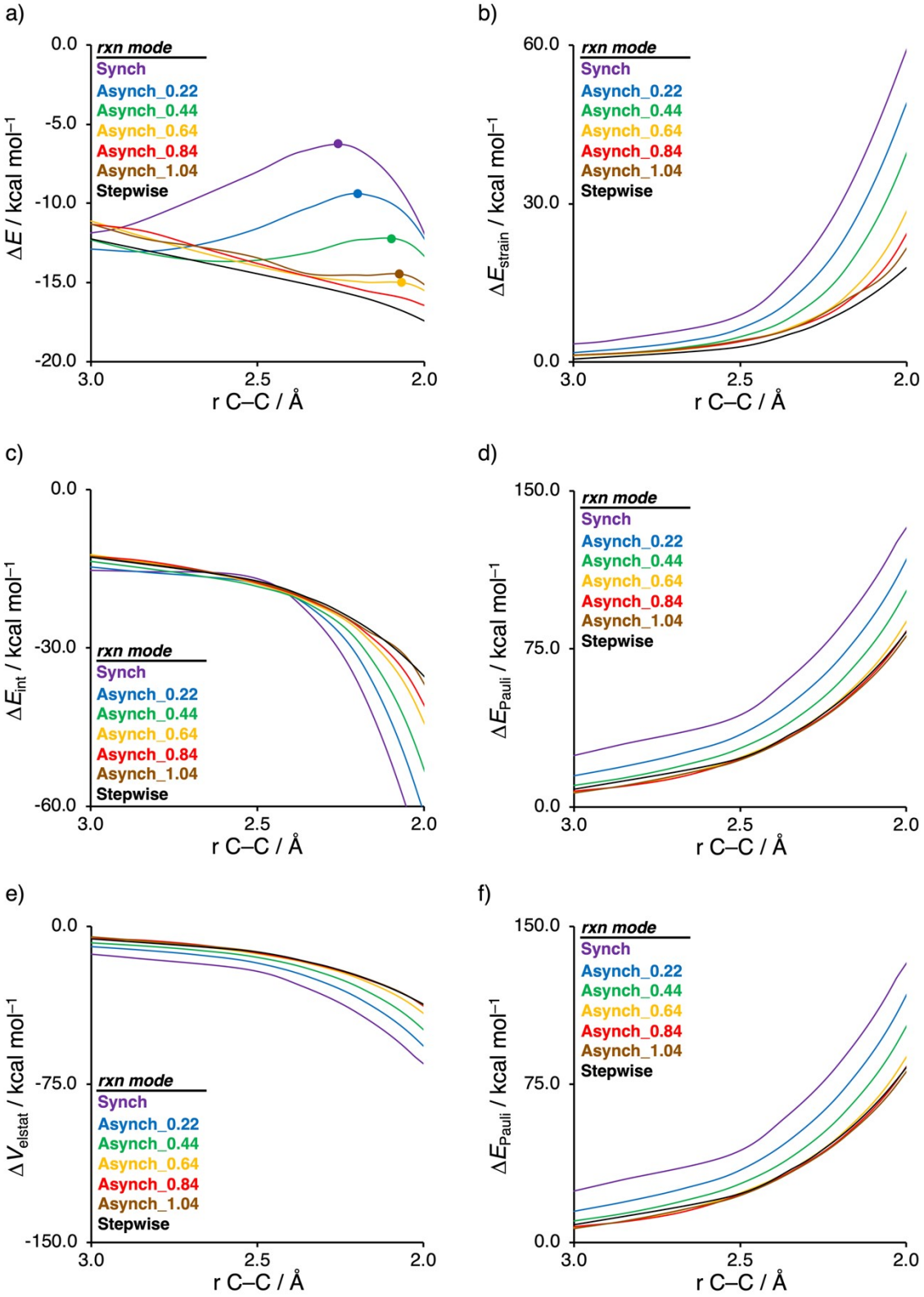

Fig. S6 Activation strain analyses of the artificially constraint synchronous, asynchronous and stepwise Diels-Alder reaction mode (rxn mode) of **B** with **O–H**$^+$ (dot indicates TS) along the IRC projected onto the shorter newly forming a $C_{\mathbf{B}}$•••C_β bond, computed at ZORA-BP86/TZ2P: (a) total energy, (b) strain energy, (c) interaction energy, (d) Pauli repulsion, (e) electrostatic interaction, and (f) orbital interactions.

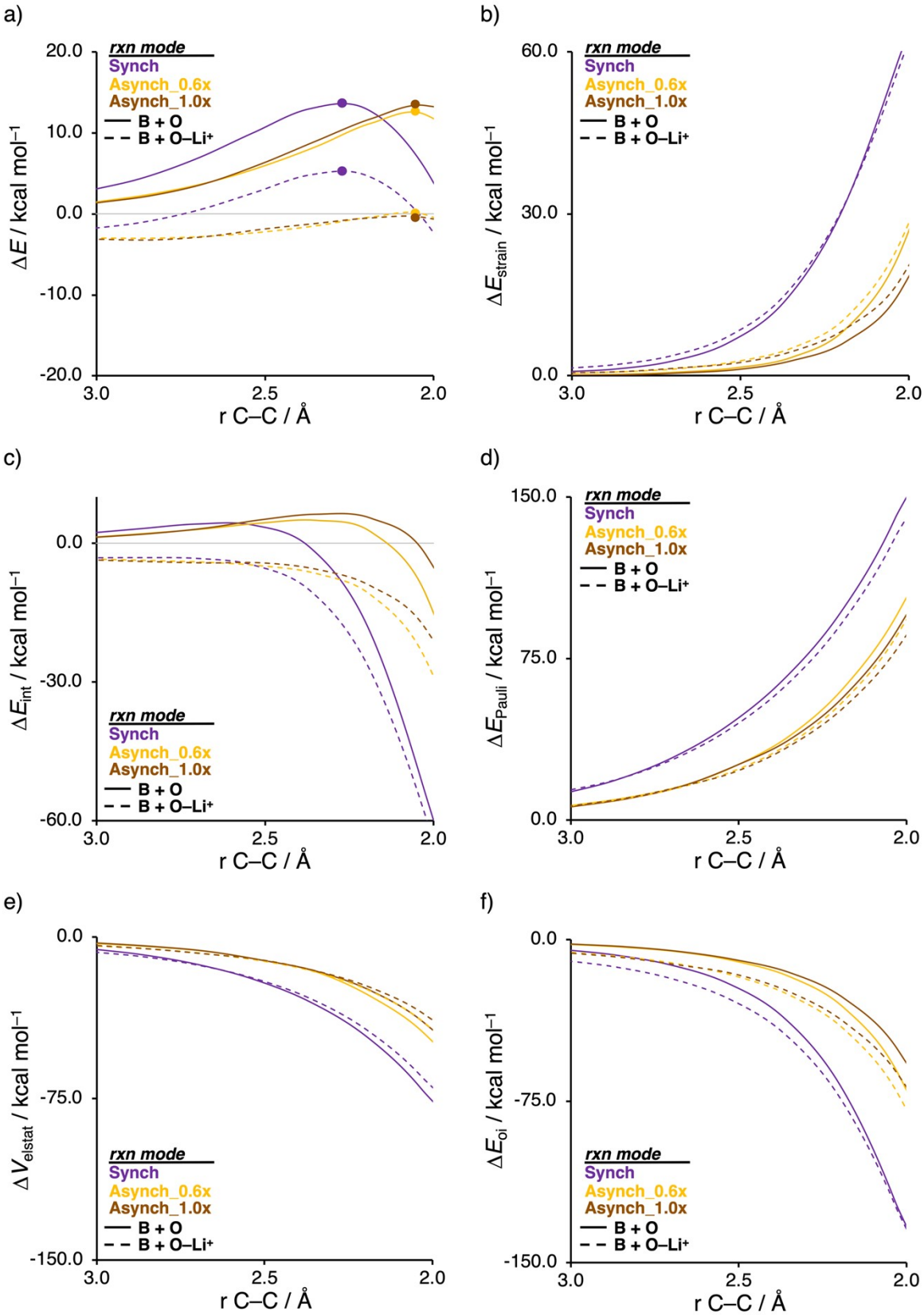

Fig. S7 Activation strain analyses of the artificially constraint synchronous, asynchronous and stepwise Diels-Alder reaction mode (rxn mode) of **B** with **O** and **O–Li**$^+$ (dot indicates TS) along the IRC projected onto the shorter newly forming a $C_{\mathbf{B}}$•••C_β bond, computed at ZORA-BP86/TZ2P: (a) total energy, (b) strain energy, (c) interaction energy, (d) Pauli repulsion, (e) electrostatic interaction, and (f) orbital interactions.

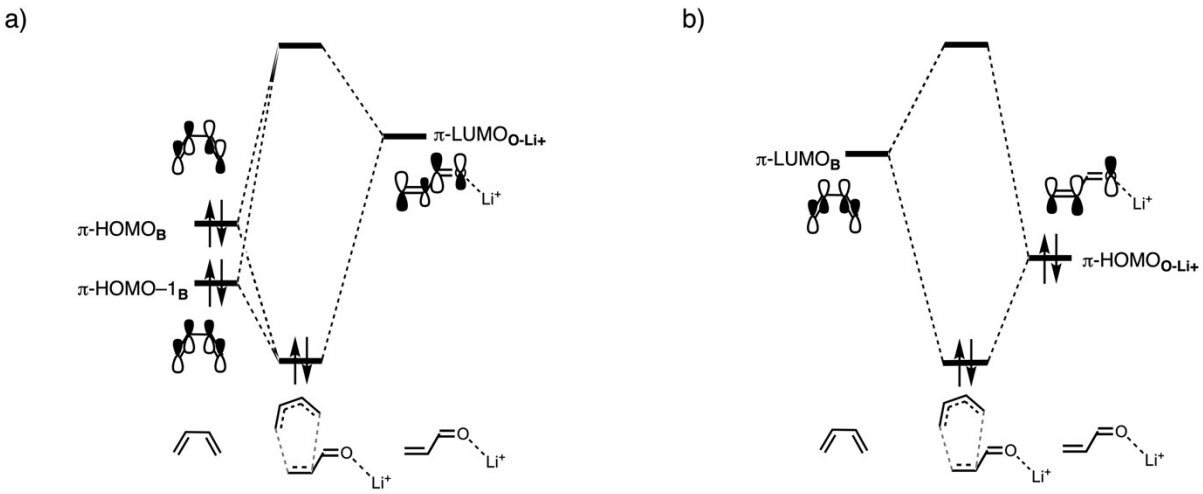

rxn mode	π-MO$_B$	⟨π-MO$_B$|π-LUMO$_{O-Li+}$⟩	ε π-LUMO$_{O-Li+}$
Synch	π-HOMO	0.18	−8.2
	π-HOMO−1	0.05	
Asynch_0.21	π-HOMO	0.17	−8.2
	π-HOMO−1	0.06	
Asynch_0.43	π-HOMO	0.16	−8.2
	π-HOMO−1	0.06	
Asynch_0.63	π-HOMO	0.14	−8.2
	π-HOMO−1	0.07	
Asynch_0.83	π-HOMO	0.13	−8.2
	π-HOMO−1	0.08	
Asynch_1.03	π-HOMO	0.12	−8.2
	π-HOMO−1	0.09	

rxn mode	⟨π-LUMO$_B$|π-HOMO$_{O-Li+}$⟩	ε π-HOMO$_{O-Li+}$
Synch	0.18	−11.9
Asynch_0.21	0.17	−11.9
Asynch_0.43	0.15	−11.9
Asynch_0.63	0.12	−11.9
Asynch_0.83	0.11	−11.9
Asynch_1.03	0.11	−11.9

Fig. S8 (a) Normal and (b) inverse electron demand orbital interaction diagrams with key overlaps and orbital energies, at consistent transition state-like geometries (shorter C_B•••C_β bond at 2.186Å), of the artificially constraint synchronous, asynchronous, and stepwise Diels-Alder reaction mode (rxn mode) of **B** with **O–Li**$^+$, computed at ZORA-BP86/TZ2P.

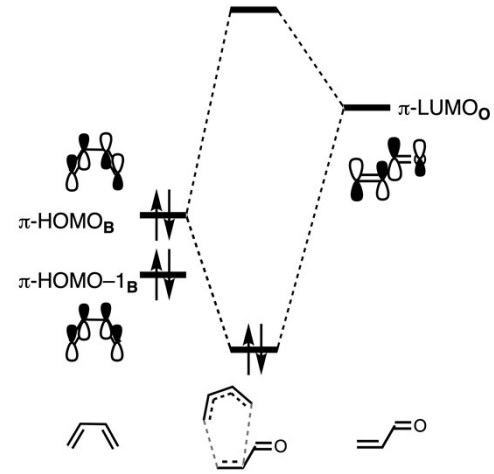

rxn mode	π-MO$_B$	⟨π-MO$_B$|π-LUMO$_O$⟩	ε π-LUMO$_O$
Synch	π-HOMO	0.22	–3.5
	π-HOMO–1	0.02	
Asynch_0.19	π-HOMO	0.20	–3.5
	π-HOMO–1	0.03	
Asynch_0.42	π-HOMO	0.18	–3.4
	π-HOMO–1	0.03	
Asynch_0.62	π-HOMO	0.16	–3.4
	π-HOMO–1	0.04	
Asynch_0.82	π-HOMO	0.15	–3.4
	π-HOMO–1	0.05	
Asynch_1.02	π-HOMO	0.14	–3.4
	π-HOMO–1	0.08	

Fig. S9 Normal electron demand orbital interaction diagrams with key overlaps and orbital energies, at consistent transition state-like geometries (shorter C_B•••C_β bond at 2.186Å), of the artificially constraint synchronous, asynchronous, and stepwise Diels-Alder reaction mode (rxn mode) of **B** with $\mathbf{O}^+$, computed at ZORA-BP86/TZ2P.

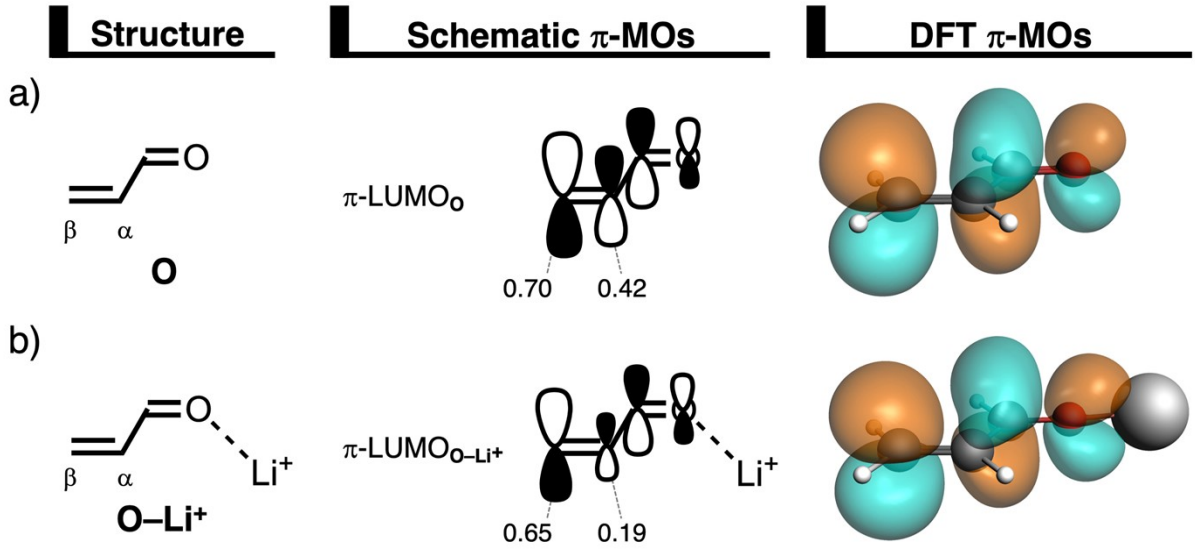

Fig. S10 Key unoccupied π-MO (isovalue = 0.03 Bohr$^{-3/2}$) computed at the equilibrium structures of (a) **O** and (b) **O–Li**$^+$, where the MO-coefficients of the carbon and oxygen 2p_z atomic orbitals, contributing to the unoccupied orbitals, are shown in the schematic π-MOs, computed at ZORA-BP86/TZ2P.

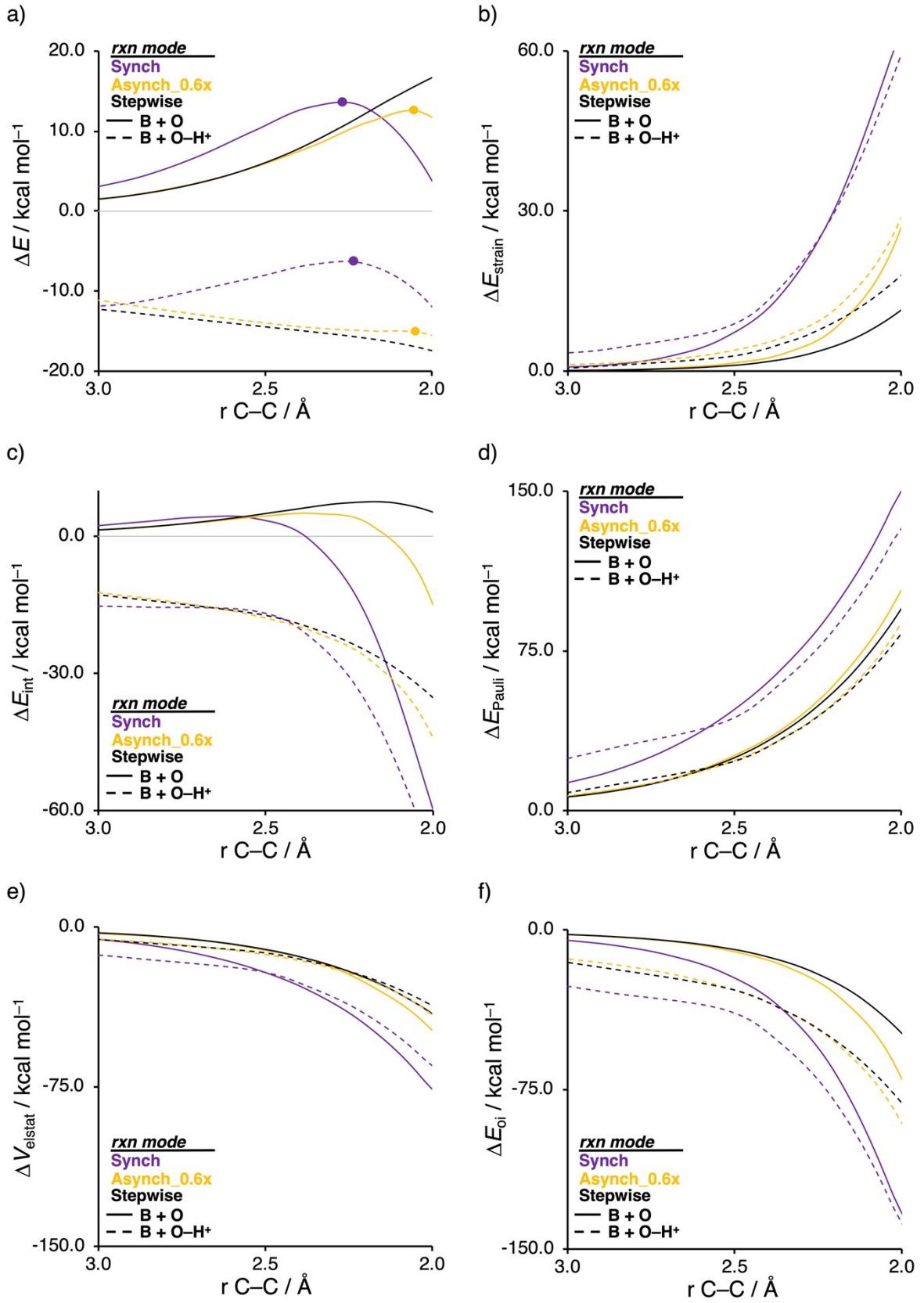

Fig. S11 Activation strain analyses of the artificially constraint synchronous, asynchronous and stepwise Diels-Alder reaction mode (rxn mode) of **B** with **O** and **O–H**$^+$ (dot indicates TS) along the IRC projected onto the shorter newly forming a $C_{\mathbf{B}}$•••C_β bond, computed at ZORA-BP86/TZ2P: (a) total energy, (b) strain energy, (c) interaction energy, (d) Pauli repulsion, (e) electrostatic interaction, and (f) orbital interactions.

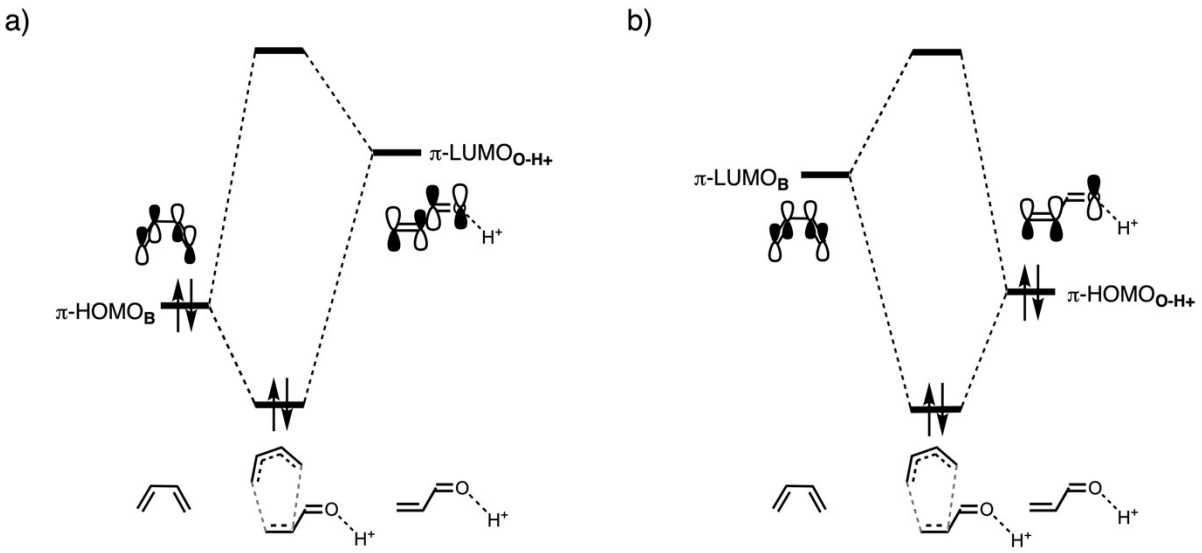

rxn mode	⟨π-HOMO$_B$|π-LUMO$_{O-H+}$⟩	ε π-LUMO$_{O-H+}$
Synch	0.17	–10.3
Asynch_0.22	0.17	–10.3
Asynch_0.44	0.16	–10.3
Asynch_0.64	0.14	–10.3
Asynch_0.84	0.13	–10.4
Asynch_1.04	0.13	–10.4
Stepwise	0.12	–10.4

rxn mode	⟨π-LUMO$_B$|π-HOMO$_{O-H+}$⟩	ε π-HOMO–1$_{O-H+}$
Synch	0.18	–13.8
Asynch_0.22	0.16	–13.8
Asynch_0.44	0.14	–13.8
Asynch_0.64	0.11	–13.9
Asynch_0.84	0.10	–13.9
Asynch_1.04	0.10	–13.9
Stepwise	0.11	–13.9

Fig. S12 (a) Normal and (b) inverse electron demand orbital interaction diagrams with key overlaps and orbital energies, at consistent transition state-like geometries (shorter C_B•••C_β bond at 2.186Å), of the artificially constraint synchronous, asynchronous, and stepwise Diels-Alder reaction mode (rxn mode) of **B** with **O–H**$^+$, computed at ZORA-BP86/TZ2P.

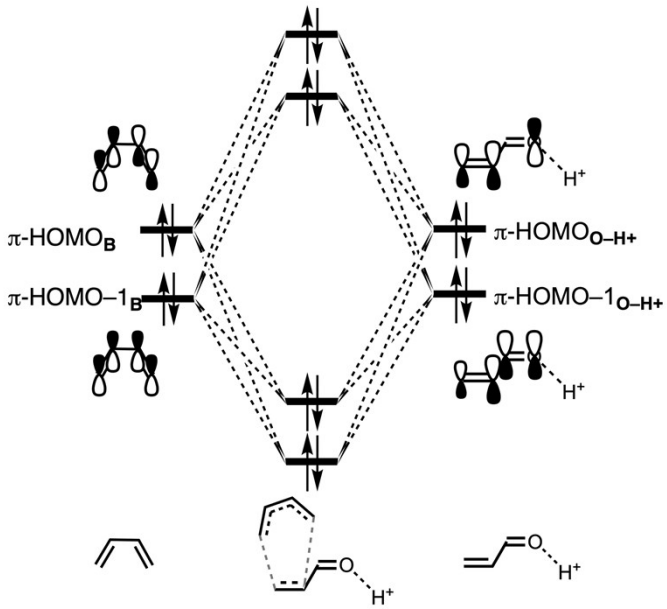

rxn mode	⟨π-HOMO$_B$|π-HOMO$_{O–H+}$⟩	⟨π-HOMO–1$_B$|π-HOMO$_{O–H+}$⟩	⟨π-HOMO–1$_B$|π-HOMO–1$_{O–H+}$⟩
Synch	0.00	0.16	0.05
Asynch_0.22	0.02	0.15	0.05
Asynch_0.44	0.04	0.14	0.05
Asynch_0.64	0.07	0.12	0.04
Asynch_0.84	0.08	0.11	0.02
Asynch_1.04	0.09	0.11	0.02
Stepwise	0.10	0.08	0.01

Fig. S13 Closed-shell orbital interaction diagrams with key overlaps, at consistent transition state-like geometries (shorter C_B•••C_β bond at 2.186Å), of the artificially constraint synchronous, asynchronous, and stepwise Diels-Alder reaction modes (rxn mode) of **B** with **O–H**$^+$, computed at ZORA-BP86/TZ2P.

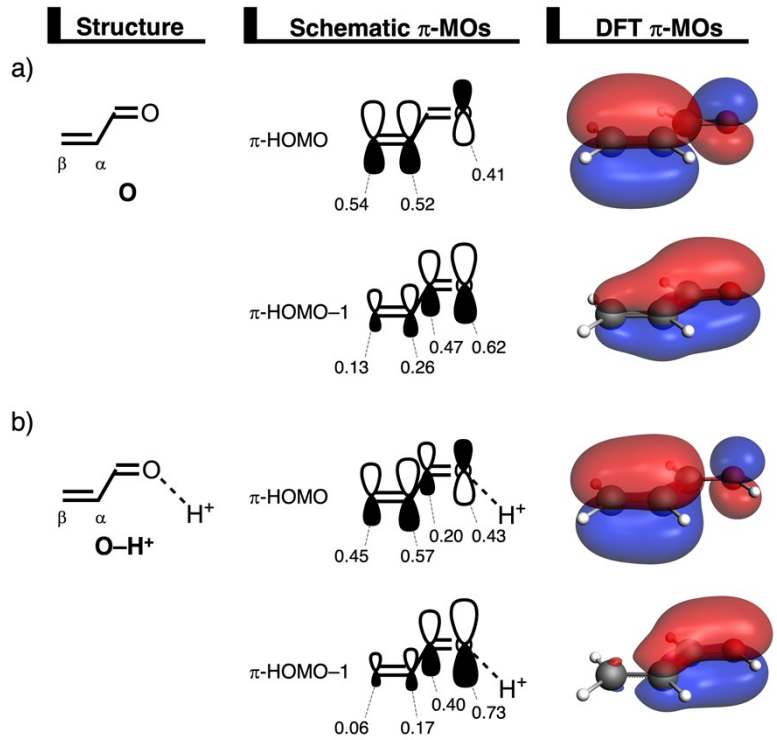

Fig. S14 Key occupied π-MOs (isovalue = 0.03 Bohr$^{-3/2}$) computed at the equilibrium structures of (a) **O** and (b) **O–H**$^+$, where the MO-coefficients of the carbon and oxygen $2p_z$ atomic orbitals, contributing to the occupied orbitals, are shown in the schematic π-MOs, computed at ZORA-BP86/TZ2P.

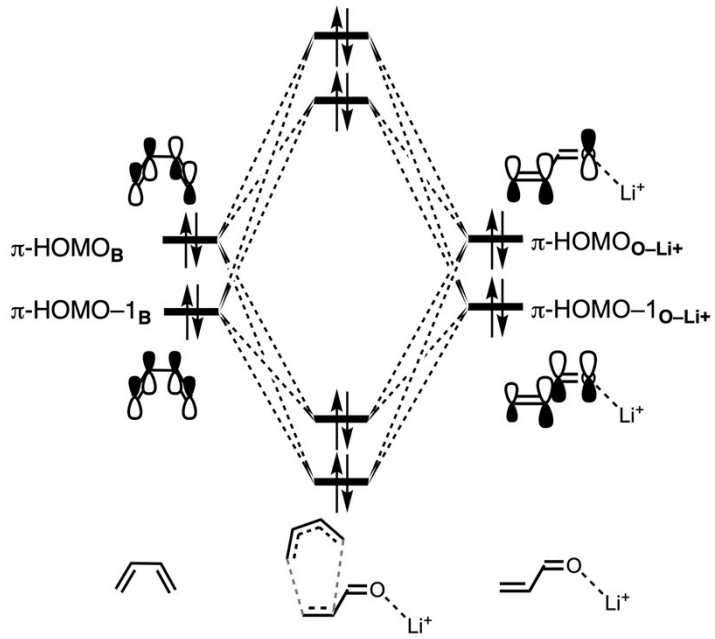

rxn mode	⟨π-HOMO$_B$|π-HOMO$_{O–Li+}$⟩	⟨π-HOMO–1$_B$|π-HOMO$_{O–Li+}$⟩	⟨π-HOMO–1$_B$|π-HOMO–1$_{O–Li+}$⟩
Synch	0.00	0.17	0.06
Asynch_0.21	0.02	0.16	0.04
Asynch_0.43	0.04	0.15	0.05
Asynch_0.63	0.07	0.13	0.05
Asynch_0.83	0.08	0.12	0.04
Asynch_1.03	0.09	0.11	0.04

Fig. S15 Closed-shell orbital interaction diagrams with key overlaps, at consistent transition state-like geometries (shorter C_B•••C_β bond at 2.186Å), of the artificially constraint synchronous, asynchronous, and stepwise Diels-Alder reaction modes (rxn mode) of **B** with **O–Li**$^+$, computed at ZORA-BP86/TZ2P.

Table S3 Cartesian coordinates (in Å), energies (in kcal mol^{-1}), and number of imaginary frequencies of all stationary points, computed at ZORA-BP86/TZ2P.

1,3-butadiene (B)
E = -1293.71
H = -1238.39
G = -1258.36
$\mathbf{N_{imag}}$ = 0

C	1.372709	-0.713395	-0.499580
C	0.701805	-0.211221	0.547604
C	-0.701805	0.211220	0.547604
C	-1.372709	0.713394	-0.499580
H	0.889339	-0.878856	-1.463378
H	2.423105	-0.989233	-0.417892
H	1.222329	-0.125437	1.506398
H	-1.222329	0.125438	1.506398
H	-0.889339	0.878856	-1.463378
H	-2.423105	0.989233	-0.417892

Acrylaldehyde (O)
E = -1079.86
H = -1039.30
G = -1059.22
$\mathbf{N_{imag}}$ = 0

O	-1.805437	-0.128643	0.000101
C	-0.681419	0.344494	0.000020
H	-0.520914	1.454121	-0.000072
C	0.558854	-0.450420	0.000033
C	1.757915	0.146949	-0.000061
H	0.445846	-1.536537	0.000121
H	2.689984	-0.416496	-0.000054
H	1.836090	1.236572	-0.000148

$AlCl_3$–Acrylaldehyde (O–$AlCl_3$)
E = -1434.84
H = -1385.54
G = -1417.50
$\mathbf{N_{imag}}$ = 0

O	0.661512	0.025306	-0.051897
C	1.905924	-0.059650	0.019823
H	2.418889	0.321265	0.922761
C	2.692720	-0.640167	-1.040494
C	4.030247	-0.709275	-0.913250
H	2.163919	-1.008038	-1.920882
H	4.659268	-1.140322	-1.690596
H	4.529909	-0.332264	-0.019317
Al	-0.547375	0.758364	1.249338
Cl	0.797970	1.373286	2.792993
Cl	-1.743858	-0.922534	1.712922
Cl	-1.447726	2.330189	0.158450

Li^+–Acrylaldehyde (O–Li^+)
E = -1001.73
H = -958.54
G = -980.98
$\mathbf{N_{imag}}$ = 0

O	0.799212	0.202108	0.348660
C	2.025686	0.024055	0.220272
H	2.701840	0.348387	1.035977
C	2.638667	-0.584087	-0.932494
C	3.978469	-0.730840	-0.969424
H	1.993175	-0.911345	-1.749145
H	4.483131	-1.185514	-1.820907
H	4.606522	-0.396611	-0.141414
Li	-0.874351	0.547703	0.739051

H^+–Acrylaldehyde (O–H^+)
E = -986.78
H = -937.74
G = -957.75
$\mathbf{N_{imag}}$ = 0

O	0.618001	0.031444	-0.043262
C	1.899998	-0.086289	-0.034326
H	2.352990	0.307356	0.882297
C	2.689077	-0.650903	-1.061715
C	4.036599	-0.699761	-0.895144
H	2.209405	-1.035759	-1.965222
H	4.686323	-1.126018	-1.659989
H	4.514715	-0.315040	0.007768
H	0.188585	-0.316764	-0.859818

TS: O + B
E = -2361.37
H = -2264.59
G = -2291.35
$\mathbf{N_{imag}}$ = 1, n = -391.095i cm^{-1}

C	-0.984945	0.969366	0.286069
C	-0.051477	1.632967	-0.508167
H	0.347730	2.584704	-0.159161
C	-2.044892	0.151645	-0.298464
O	-3.075323	-0.188802	0.272101
H	-1.866135	-0.126365	-1.370893
H	-1.112862	1.242784	1.335295
H	-0.144688	1.548578	-1.591315
C	0.171966	-1.246589	0.877796
C	0.854625	-1.463843	-0.292425
C	1.702813	-0.498494	-0.877605
C	1.864892	0.773308	-0.342725
H	2.486204	1.494146	-0.874279
H	-0.593770	-1.940668	1.219214
H	0.610925	-2.349423	-0.883038
H	2.062548	-0.687178	-1.891227
H	0.498726	-0.505853	1.602924
H	1.833905	0.915851	0.736306

P: O + B
E = -2409.61
H = -2309.97
G = -2335.91
$\mathbf{N_{imag}}$ = 0

C	-0.591977	-0.109794	-0.417378
C	0.740295	0.005527	-1.192978
H	0.554100	0.369258	-2.213001
C	-1.548123	-0.998101	-1.177552
O	-2.608033	-0.650478	-1.656805
H	-1.196486	-2.060835	-1.286574
H	-1.053708	0.885308	-0.334941
H	1.188224	-0.997325	-1.283325
C	-0.337115	-0.687748	0.991389
C	0.866950	-0.075970	1.657170
C	1.775085	0.665679	1.013421
C	1.719020	0.937080	-0.465611
H	2.724929	0.828288	-0.900588
H	-0.209329	-1.784891	0.929841
H	0.976170	-0.253073	2.729663
H	2.606766	1.101253	1.571714
H	1.438307	1.991085	-0.637629
H	-1.227981	-0.531377	1.619211

TS: O–$AlCl_3$ + B
E = -2725.09
H = -2620.02
G = -2656.62
$\mathbf{N_{imag}}$ = 1, n = -289.409 cm^{-1}

C	-1.270422	-1.342160	-0.419335
C	-2.564712	-1.703977	-0.787237
C	-0.432752	-0.623739	-1.303490
O	0.804662	-0.380418	-1.150239
H	-0.865255	-0.300591	-2.266089
Al	2.093779	-0.332827	0.176152
Cl	1.442018	-1.584127	1.798296
Cl	2.058481	1.741878	0.707423
Cl	3.856530	-1.015856	-0.779296
H	-0.839892	-1.673798	0.527727
H	-3.023510	-2.561156	-0.296020
H	-2.893373	-1.533964	-1.812234
C	-1.677477	1.423191	0.343245
C	-2.759139	1.600996	-0.467480
C	-3.870220	0.714682	-0.517920
C	-3.965946	-0.463122	0.203891
H	-4.866295	-1.067788	0.102583
H	-0.792716	2.055157	0.269755
H	-2.736371	2.412356	-1.197826
H	-4.616615	0.899613	-1.294023
H	-3.439668	-0.575638	1.149934
H	-1.677178	0.706924	1.162703

P: O–$AlCl_3$ + B
E = -2762.86
H = -2654.50
G = -2692.34
$\mathbf{N_{imag}}$ = 0

C	-1.371561	0.116758	-0.454102
C	-2.125160	-1.241993	-0.615992
C	-0.161441	0.059146	-1.296134
O	1.018316	0.001998	-0.912620
H	-0.314895	0.038325	-2.393458
C	-2.283272	1.287010	-0.900322
C	-3.676704	1.147607	-0.347959
C	-4.153201	0.025897	0.200655
C	-3.363203	-1.250120	0.288654
H	-4.000579	-2.102703	0.007553
Al	1.849650	-0.004602	0.826193
Cl	1.016428	-1.759373	1.704302
Cl	3.903033	-0.090766	0.351579
Cl	1.157040	1.823450	1.671179
H	-1.084453	0.242068	0.598855
H	-1.456289	-2.071868	-0.356627
H	-2.428776	-1.362571	-1.667155
H	-2.318567	1.348096	-2.003285
H	-4.303539	2.040204	-0.394514
H	-5.163592	0.017222	0.613757
H	-3.063728	-1.434984	1.333910
H	-1.839560	2.233804	-0.559077

RC: O–Li^+ + B
E = -2299.56
H = -2199.71
G = -2232.73
$\mathbf{N_{imag}}$ = 0

C	-1.112844	-1.647494	0.181177
C	-2.333170	-2.143970	-0.143491
C	-0.279611	-1.062827	-0.824537
O	0.912274	-0.712881	-0.637908
H	-0.707653	-0.964269	-1.839235
Li	2.587655	-0.310393	-0.585032
H	-1.842981	1.270417	0.771410
H	-4.788117	0.199292	-1.498161
H	-3.684542	0.036199	1.381030
H	-0.715879	-1.720683	1.195243
H	-2.945914	-2.676695	0.580922
H	-2.701683	-2.111106	-1.167901
C	-1.952010	1.649419	-0.244850
C	-3.000922	1.326374	-1.028012
C	-4.084181	0.414183	-0.690290
C	-4.295424	-0.180425	0.504888
H	-5.150429	-0.837370	0.656204
H	-1.199947	2.358185	-0.587954
H	-3.055237	1.772402	-2.023928

TS: O–Li$^+$ + B
E = -2297.30
H = -2197.67
G = -2227.42
$\mathbf{N_{imag}}$ = 1, n = -264.495i cm^{-1}

C	-1.274191	-1.371044	-0.250009
C	-2.545800	-1.686449	-0.731363
C	-0.323324	-0.684604	-1.036224
O	0.902484	-0.552789	-0.736626
H	-0.662166	-0.297030	-2.015135
Li	2.597701	-0.508357	-0.585371
H	-4.583114	0.815694	-1.446303
H	-1.804036	0.841151	1.200285
H	-3.536381	-0.509553	1.139526
H	-0.953021	-1.734514	0.728539
H	-3.066372	-2.540251	-0.299137
H	-2.776122	-1.498303	-1.779037
C	-1.793408	1.539735	0.366380
C	-2.817544	1.629121	-0.523926
C	-3.886382	0.689636	-0.614493
C	-4.005004	-0.451579	0.158761
H	-4.885817	-1.079078	0.030556
H	-0.961265	2.241091	0.330540
H	-2.789587	2.419347	-1.276473

P: O–Li$^+$ + B
E = -2331.55
H = -2229.38
G = -2258.02
$\mathbf{N_{imag}}$ = 0

C	-1.411214	0.091952	-0.317946
C	-2.162633	-1.253539	-0.581581
C	-0.128740	0.067402	-1.039555
O	0.993862	0.111467	-0.512477
H	-0.181627	-0.008224	-2.146267
C	-2.282992	1.275481	-0.828340
C	-3.708158	1.143762	-0.359158
C	-4.233350	0.014508	0.123757
C	-3.472839	-1.278390	0.215500
H	-4.096169	-2.102160	-0.164511
Li	2.641724	0.182507	0.078613
H	-5.267043	0.008665	0.472498
H	-3.275631	-1.523347	1.272811
H	-1.856042	2.222332	-0.465764
H	-1.221487	0.201062	0.759627
H	-1.529774	-2.106833	-0.304435
H	-2.377477	-1.334101	-1.657473
H	-2.246990	1.327050	-1.930907
H	-4.314991	2.048833	-0.418113

Int: O–H$^+$ + B
E = -2300.52
H = -2194.09
G = -2223.07
$\mathbf{N_{imag}}$ = 0

C	-0.116018	-1.329606	-0.165990
C	-1.400561	-1.179303	0.531051
H	-1.926786	-2.130198	0.668503
C	0.233697	-0.532740	-1.210334
O	1.345225	-0.620213	-1.945635
H	-0.415580	0.267589	-1.572176
H	0.575624	-2.103869	0.178816
H	-2.061640	-0.477231	0.010671
C	-2.077850	2.231618	2.783758
C	-2.849440	1.109895	2.881053
C	-2.394211	-0.202418	2.613315
C	-1.126357	-0.607330	2.065973
H	1.925586	-1.343193	-1.633320
H	-2.491851	3.213502	3.010643
H	-3.885236	1.215100	3.208283
H	-3.126709	-1.001173	2.769891
H	-0.716866	-1.478909	2.593325
H	-1.029601	2.198367	2.486720
H	-0.377026	0.186808	2.010720

TS: O–H$^+$ + B
E = -2300.00
H = -2194.13
G = -2221.31
$\mathbf{N_{imag}}$ = 1, n = -49.296i cm^{-1}

C	-1.299393	-0.627633	-1.305275
C	-1.010280	-0.584619	0.130926
H	-1.521806	-1.361703	0.708771
C	-1.741209	0.463969	-1.987148
O	-2.088396	0.515076	-3.274856
H	-1.883157	1.432033	-1.501634
H	-1.153705	-1.573817	-1.834563
H	-1.274015	0.387622	0.563538
C	2.312837	1.578848	-0.161860
C	1.772875	1.273583	1.053171
C	1.042300	0.091582	1.325022
C	0.616557	-0.903299	0.379299
H	0.652241	-1.918759	0.787057
H	2.850235	2.514321	-0.313801
H	1.909909	1.972877	1.879640
H	0.680441	-0.027489	2.351093
H	2.242336	0.909411	-1.019033
H	1.125444	-0.864668	-0.585937
H	-1.983170	-0.354642	-3.710418

P: O–H$^+$ + B
E = -2319.13
H = -2211.37
G = -2237.64
N$_{imag}$ = 0

C	-1.439060	-0.020867	-0.376903
C	-2.117330	-0.199402	1.044735
C	-0.049657	-0.380647	-0.299925
O	0.955186	0.399593	-0.488268
H	0.265065	-1.403012	-0.056268
C	-2.190446	-0.975604	-1.380391
C	-3.660233	-0.662385	-1.341980
C	-4.270501	-0.085564	-0.301024
C	-3.561901	0.303441	0.962000
H	-4.099751	-0.117134	1.828027
H	0.687283	1.322818	-0.711648
H	-3.611039	1.396601	1.095207
H	-5.334905	0.144172	-0.359834
H	-1.794476	-0.829167	-2.394748
H	-1.554319	1.026258	-0.702344
H	-1.555852	0.352710	1.807545
H	-2.088036	-1.265844	1.303600
H	-1.988425	-2.022143	-1.103645
H	-4.218901	-0.891448	-2.250845